

# International Conference on Space Optics—ICSO 2022

Dubrovnik, Croatia

3–7 October 2022

*Edited by Kyriaki Minoglou, Nikos Karafolas, and Bruno Cugny,*



***The art of characterizing light scattering from optical components  
and systems***



# The art of characterizing light scattering from optical components and systems

Marcus Trost, Yusuf Sekman, Anne-Sophie Munser, Alexander Bergner, Nils Rommel,  
Tobias Herffurth, Paul Böttner, Matthias Goy

Fraunhofer Institute for Applied Optics and Precision Engineering, Albert-Einstein-Straße 7, 07745 Jena, Germany

## ABSTRACT

Even high-end optical components exhibit small amounts of imperfections, which can easily limit the performance of optical systems with respect to imaging contrast, optical throughput, imaging ghosts, and increased light scattering. Characterizing the scattering properties of optical components is thus an important step during the development of sophisticated optical systems as well as to identify and steadily improve materials as well as manufacturing and assembling steps. This is illustrated for different optical components as well as optical systems. Furthermore, different characterization concepts are discussed, which allow overcoming typical limits for angles resolved light scattering measurements, such as scattering very close to the specular beam directions (off specular scattering angles  $< 0.1^\circ$ ) or measurements in retro-reflection, which are important for gratings used in Littrow configuration or optical mirrors for laser-based communication.

**Keywords:** Light scattering, grating, mirror, optical system, near angle scattering, aberrations, time resolved measurements

## 1. INTRODUCTION

Light scattering can critically affect the performance of high-end optical systems. For instance, unavoidable but even small residual imperfections of optical components such as surface or coating roughness, bulk inhomogeneities, defects, contaminations, as well as the interaction of light with apertures and baffles give rise to light scattering propagating through the optical system, which degrades the imaging quality and leads to a loss of the optical throughput. An example for this is shown in Figure 1.

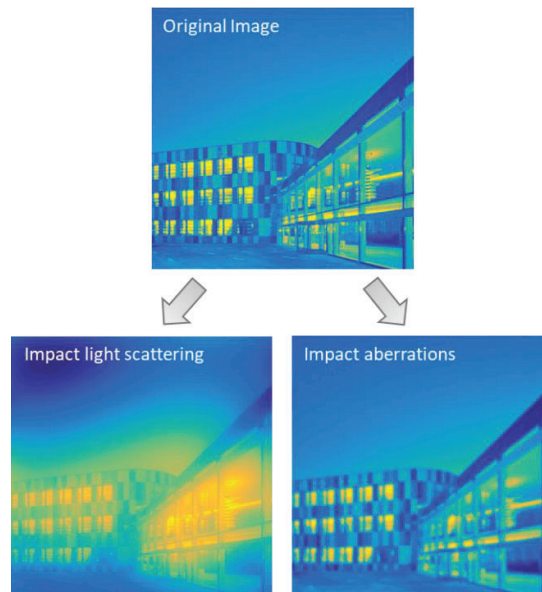


Figure 1: Simulated impact of form deviations (aberrations) and surface roughness/contamination induced scattering on optical performance of a Double-Gauss camera lens.

Shape deviations and aberrations of the optical components used in an optical system cause a reduced resolution. Light scattering on the other hand preserves the resolution, however, introduces a reduced contrast or foglike imaging.

Measurements of the angle resolved scattering provide essential information on the suitability of optical components in an optical system. Especially in complex optical systems and for high-end applications, knowledge about the scattering properties of the optical elements is fundamental in order to assess their impact onto the optical performance of the system.

Light scattering can be characterized with the help of scatterometers [1-7], which use 3D goniometers to detect the angle resolved scattering at arbitrary angles of incidence and at various scattering angles and thus naturally exhibit many degrees of freedom. Nevertheless, also these systems can face measurement scenarios, which are quite challenging. This includes:

- Light scattering measurements in direct vicinity of the specular or diffracted beam. An illustrative example where this is of high relevance is the detection of exoplanets close to a bright star, which exhibit orders of magnitude differences in their light signal. Thus, even small amounts of light scattering in the imaging system can outshine the weak signal from the exoplanet.
- Light scattering measurements in retro-reflection or in other words the direction from which the incoming light beam is illuminating the sample. This is important for gratings used in Littrow configuration of laser-based communication terminals that share their receiver and transmitter optics, as any retro-reflected light will cause false communication signals.
- Light scattering measurement of assembled optical groups. Examples for this are three mirror anastigmats (TMAs), grisms or prism-grating-prisms (PGPs). All these optical systems exhibit entrance and exit pupils at different planes, requiring an independent illumination from the actual scatterometer.

In the following, different measurement approaches are introduced that allow to overcome these challenges and at the same time provide practical measurement concepts.

## 2. LIGHT SCATTERING QUANTITIES

One of the oldest definitions for angle resolved scattering is the Bi-directional Scattering Distribution Function (BSDF) [8], which is defined as the ratio of the scattered radiance  $L$  in the direction of the polar  $\theta_s$  and azimuthal  $\varphi_s$  scattering angles (see Figure 2) and the irradiance  $E$  that is illuminating the sample surface:

$$\text{BSDF}(\theta_i, \theta_s, \varphi_s, \lambda) = \frac{dL(\theta_s, \varphi_s)}{dE(\theta_i)} \quad (1)$$

Besides the two scattering angles, the BSDF also depends on the angle of incidence,  $\theta$ , the light wavelength,  $\lambda$ , and the polarization of the incident and scattered light and is thus a multidimensional function. In order to differentiate more easily between forward and backward scattering, the two expressions: Bi-directional Reflectance Distribution Function (BRDF) and Bi-directional Transmittance Distribution Function (BTDF) are commonly used.

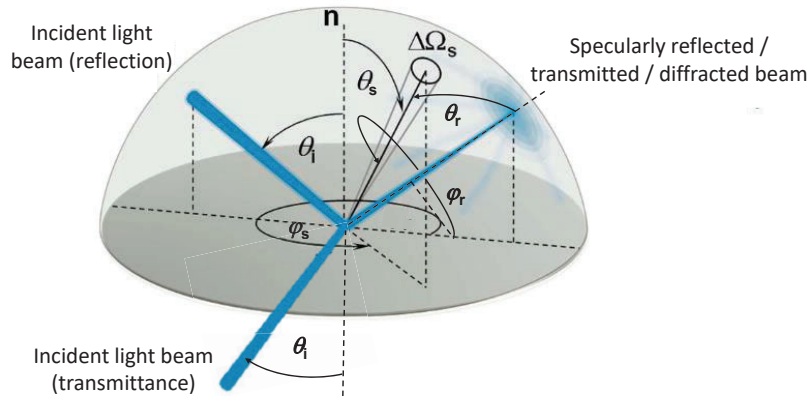


Figure 2: Scattering geometry.

Rather than measuring radiometric quantities, usually the incident,  $P_i$ , and scattered,  $P_s$ , light power are measured during a scattering measurement, which leads to the definition of the angle resolved scattering, ARS, which was also recently standardized [9-11]:

$$ARS(\theta_i, \theta_s, \varphi_s, \lambda) = \frac{\Delta P_s(\theta_s, \varphi_s)}{\Delta \Omega_s P_i} = BSDF(\theta_s, \varphi_s) \cos \theta_s \quad (2)$$

The ARS is directly connected to the BSDF, however, avoids the singularity at  $\theta_s = \pm 90^\circ$ . In order to realize a measurement system independent quantity, the power ratio is divided by the detector solid angle  $\Delta \Omega$ . The coordinate origin for all angles lies at the exit surface for transmissive scattering and at the entrance surface for reflective scattering measurement, which might not seem to be too much of a difference but can cause larger differences for a fiber.

Integrating the ARS allows determining the Total scattering, TS:

$$TS_{b/f} = \int_0^{2\pi} \int_{2^\circ/95^\circ}^{85^\circ/178^\circ} ARS(\varphi_s, \varphi_s) \sin \varphi_s d\theta_s d\varphi_s \quad (3)$$

in the backward,  $TS_b$ , and forward,  $TS_f$ , scattering hemispheres. According to the ISO standard 13696 [12], the specular beam is excluded in the calculation within an opening angle of  $\theta_r = \pm 2^\circ$ , which allows TS values to be treated as a loss factor similar to an absorption loss,  $A$ . The energy balance thus reads:

$$1 = R + T + A + TS_b + TS_f \quad (4)$$

### 3. MEASUREMENT SYSTEMS

Various instruments for angle resolved scatter measurements have been developed at Fraunhofer IOF together with analysis techniques to link the measured light scattering distributions to the corresponding surface or thin film properties [5-7, 13-15]. This includes systems for different spectral regions, starting in the extreme ultraviolet at 13.5 nm and ranging to the far infrared at 10.6  $\mu\text{m}$ . Also, spectrally tunable scatterometers between 192 nm and 2.7  $\mu\text{m}$  with bandwidth down to 0.1 nm have been realized.

Figure 3 shows the scatterometer MLS10, which is designated for the ultraviolet, visible, and infrared spectral range. The system exhibits more than 14 motorized degrees of freedom to realize arbitrary angles of incidence and scattering in the backward and forward direction at different sample positions. The scatterometer can handle sample sizes of up to 600 mm.

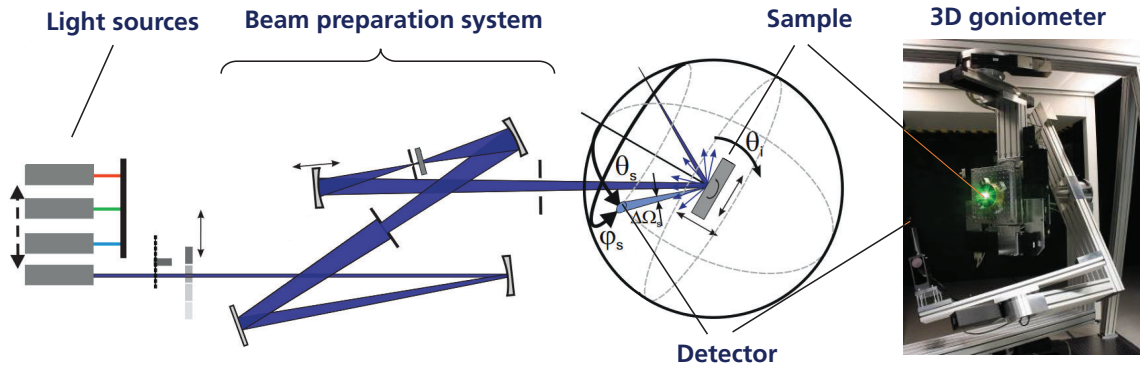


Figure 3: Scatterometer MLS10 for angle resolved light scattering measurements in the UV-VIS-IR range.

An example of the large linearity and dynamic range of this system is illustrated in Figure 4, which shows an angle resolved scattering measurement of a highly reflective mirror designed for a wavelength of 1064 nm, which exhibits a nominal reflectance of 99.999%.

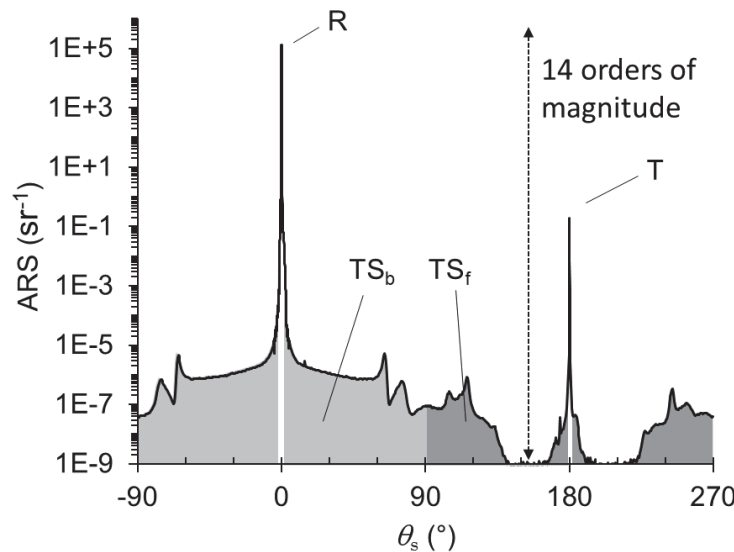


Figure 4: Light scattering measurement of a highly reflective mirror at an angle of incidence of 0°. The scattering angle  $\theta_s = 0^\circ$  corresponds to the direction of the reflected beam. The specular transmitted light direction corresponds to  $\theta_s = 180^\circ$ .

The large dynamic range also allows determining the residual transmittance of  $T = 1.5$  ppm, which is beyond the measurement range of a typical spectrophotometer. The scattering losses are as low as  $TS_b = 5.9$  ppm and  $TS_f = 0.6$  ppm. Based on Eq. (4), the resulting Reflectance (+ absorption) is  $R + A = 99.9992\%$ , which perfectly matches nominal reflectance as well as the results from cavity ringdown measurements ( $R_{\text{Cavity ringdown}} = 99.992 \pm 0.006\%$ ) [16].

A different measuring approach for angle resolved scattering measurements is shown in Figure 5. Here, the focus was less on high degrees of freedom, which resulted in the fixed angle of incidence of  $18^\circ$  and a wavelength of 650 nm. This simplification enables a compact design that can be used for in-process characterization or together with a robot for a quick inspection of large and complex shaped sample geometries with respect to its surface roughness, homogeneity, defects, and particles as illustrated in Figure 6.

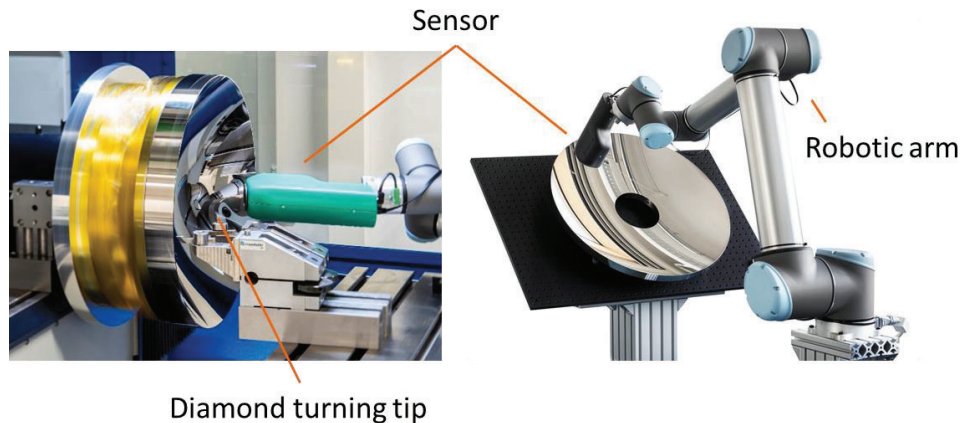


Figure 5: Light scattering sensor horos during roughness characterization within a diamond turning machine (left) and characterization of a primary mirror of a Cassegrain telescope (right).

The sensor [13] is based on a matrix array, which allows characterizing the ARS in a cone of  $\pm 8^\circ$  around the specularly reflected light in less than 1 second. Together with first order vector perturbation scattering theories [1], it is possible to determine the surface roughness over the entire clear aperture of an optic even for freeform surfaces with the help of a robotic arm. The resulting roughness maps provide direct feedback about contaminations and defects and the corresponding scattering distributions directly show the impact of these imperfections on the optical performance [17].

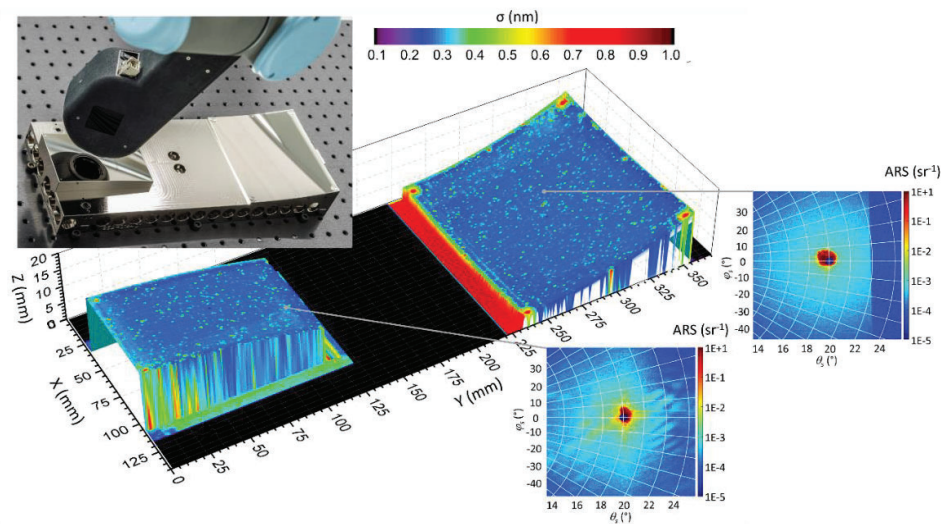


Figure 6: Light scattering based roughness and defect/particle characterization of two mirrors of a TMA.

## 4. PUSHING THE LIMITS OF SCATTEROMETERS

### 4.1. Near angle measurements

A challenge for scatterometers and light scattering sensors is the detection of scattered light very close to the specular beam direction such as the reflected, transmitted, or diffracted beam. Other than in a ray-tracing simulation where the specular beam can be represented by a single infinitesimal small ray, real world measurements struggle with the size of the probe beam. Therefore, scatterometers usually focus the incident light beam not on the sample but on the detector plane such that a detector can pick up the scattering signal very close to the specular direction at angles smaller than  $\theta_i = 1^\circ$  [18]. As the scattering of an optical component quickly increases towards the specular beam direction, there

is always the wish to measure at even smaller off-specular scattering angles, which requires a needle-like probe beam.

Nevertheless, the optics used within the illumination part of a scatterometer underly physical laws and exhibit scattering and cause aberrations, which broaden the needle-like probe beam. Also, the optical element under test can cause additional aberrations. An example for this is shown in Figure 7, which shows the aberrations introduced by a plane grating. Similar aberrations also occur for curved optics.

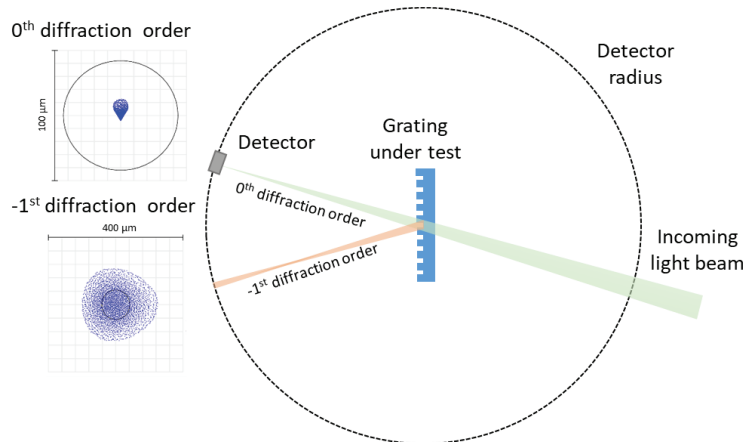


Figure 7: Probe beam size at the detector plane for different diffraction orders of a plane grating. The incoming light is focused on the detector plane. Thus, for the 0<sup>th</sup> diffraction order, a diffraction limited spot can be realized (the black circle in the spot diagrams on the left shows the Airy disc). The small variation of the angles of incidence due to convergent incoming light beam leads to a broadening of the spot diagram for the -1<sup>st</sup> diffraction order beyond the Airy disc.

The slightly converging probe beam necessary to prevent an extended Gaussian beam at the detector plane together with the grating, leads to a broadening of the diffraction order. Thus, extending the detector radius in order to increase the mechanical angular resolution is not an option to measure at smaller off-specular scattering angles. Also reducing the detector radius is not improving the situation significantly to compensate for a possible defocus. Instead, the aberrations caused by the sample under test need to be compensated by the illumination optics, as illustrated in Figure 8.

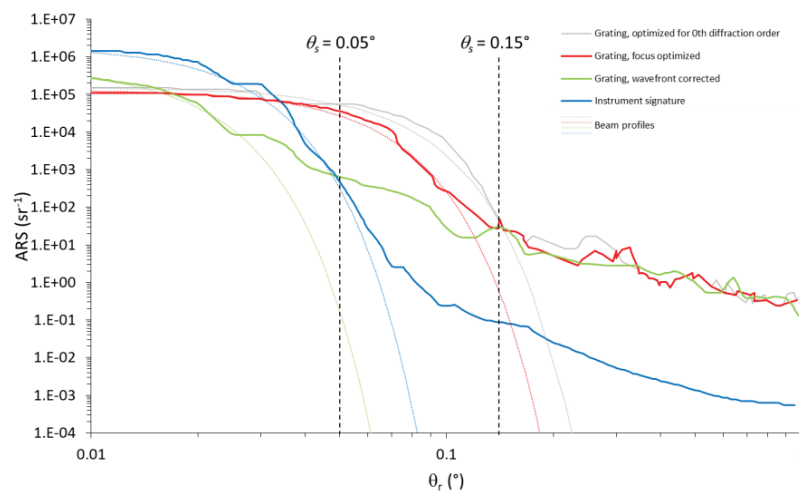


Figure 8: Near angle measurements of the -1<sup>st</sup> diffraction order of a plan grating (grating period: 1200 lines/mm) performed with the scatterometer MLS10 at a wavelength of 633 nm.

The graph also shows the instrument signature, which is a scattering measurement without a sample. Thus, the curve indicates the intrinsic scattering and aberrations of the scatterometer and with this provides a limit to which angles the scattering of a sample can be characterized. In order to reduce the instrument signature as much as possible, the optics used in a scatterometer have to be of a very good quality, similar if not better than the optic under test.

Between the focused and defocused states, the extension of the Gaussian beam shape (indicated by the dashed lines) limits the accessible scattering angle to about  $\theta_s > 0.15^\circ$ . Only if the aberrations introduced by the grating are compensated by the illumination optics of the scatterometer, the extension of the Gaussian probe beam reduces significantly enabling light scattering measurement as close as  $\theta_s = 0.05^\circ$  to the diffraction order.

The exact limit of course depends on the scattering level of the sample under test. But, even for well-polished mirror surfaces with an rms-roughness  $\sigma < 0.2$  nm, it is possible to characterize the scattering as close as  $0.07^\circ$  to the specular direction, if aberrations introduced by the sample are compensated as illustrated in Figure 9.

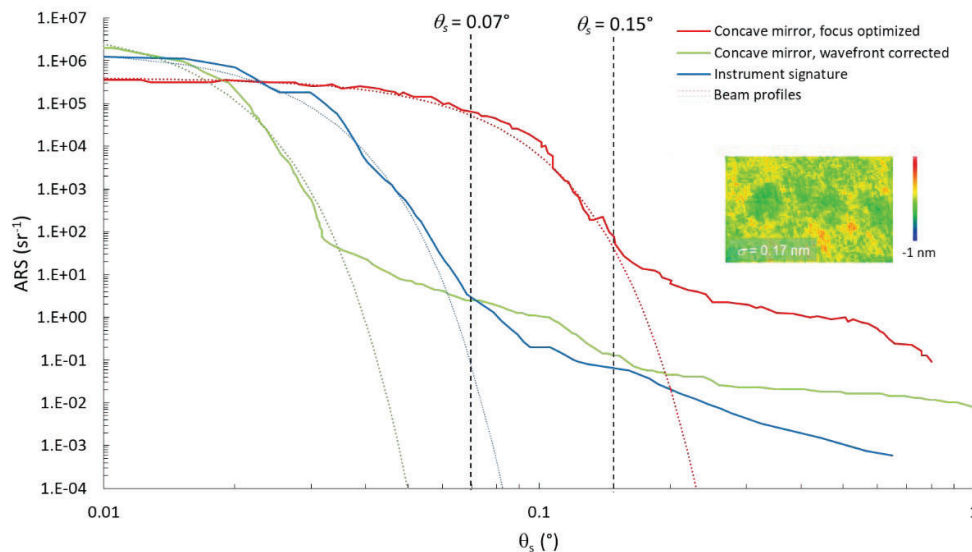


Figure 9: Near angle measurements of a concave mirror (focal length: 500 mm, form errors  $< \lambda/40$ ) at a wavelength of 633 nm. The inset shows the surface topography of the mirror within a scan size of  $140 \times 105 \mu\text{m}^2$ .

## 4.2. Retro-reflection measurements

The freely positional detector of a scatterometer also leads to scenarios in which the detector blocks the incident light beam. Thus, no scattered light can be measured at these positions, as illustrated in Figure 10. Unfortunately, this retro-reflection direction is relevant to many applications. Typical examples include cavity mirrors for laser or mirrors used for laser-based communication in which the signal of a transmitter is partly reflected into the receiving optics, which lowers the signal to noise ratio. Another example are gratings used in Littrow configuration.

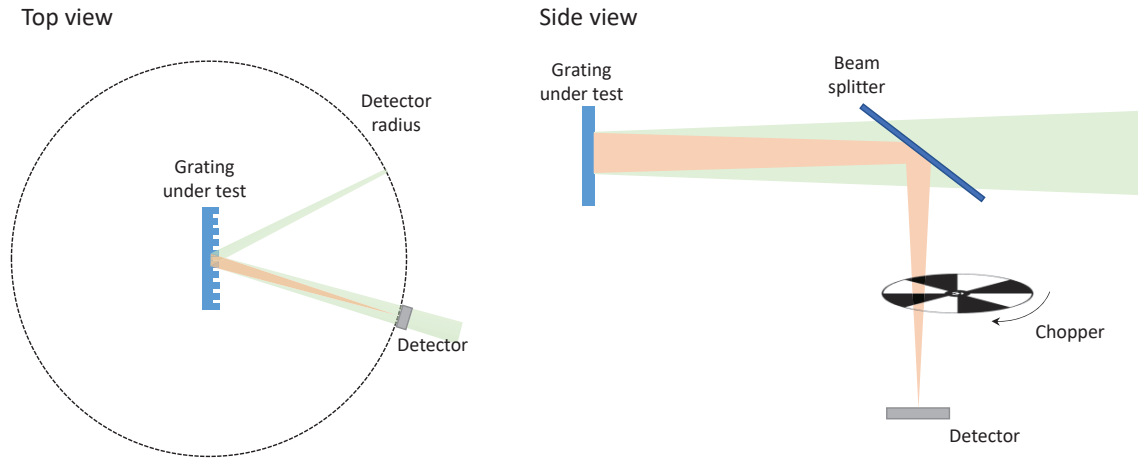


Figure 10: Light scattering measurements in retro-reflex direction. Left: Characterization of the use order of a grating used in Littrow configuration; right: beam splitter at detector position, which allows illuminating the sample and simultaneous detection of the scattered light without any obscurations from the detector.

To overcome this challenge, partial reflectors were used at the detector position in the past to transmit light to the sample under test and reflect the scattered light to a detector. In order to differentiate between the incoming and scattered light, the scattered light is modulated with a chopper directly in front of the detector to allow for lock-in amplification. However, the scattering at the chopper blades and the high signal difference between the incoming and scattered light usually limits the sensitivity quite drastically.

Another approach is given by using short laser pulses as illustrated in Figure 11. The time resolved scattering signal of a nanosecond laser pulse exhibits several peaks, which can be assigned to different scattering events: a) the scattering of the incoming light beam at the partial reflector and b) the scattering of the sample. Analyzing the second peak, thus, allows characterizing the scattering distribution in the retro-reflection direction despite the also present further scattering signals. This way, the scattering around the use order of a grating in Littrow configuration can be characterized.

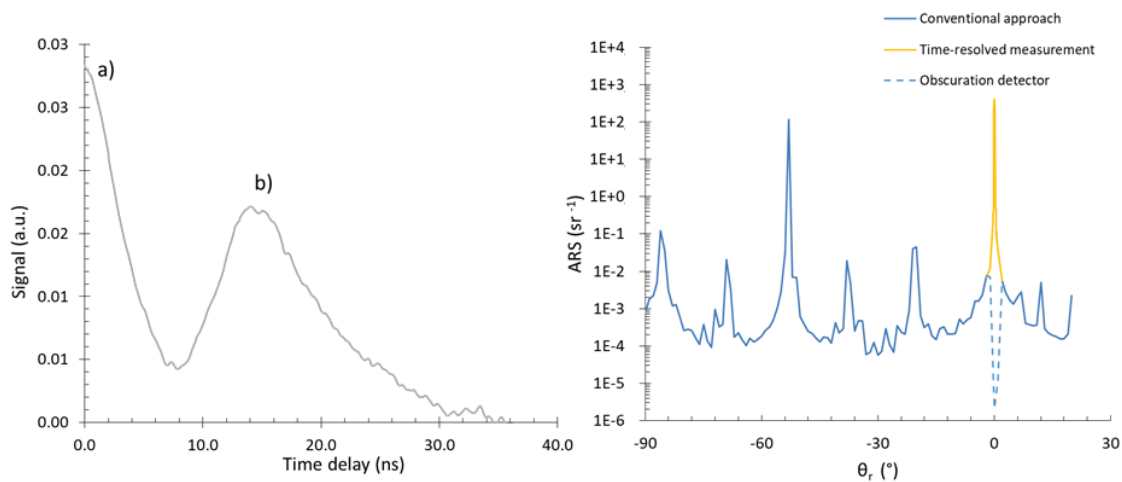


Figure 11: Time resolved light scattering measurements: Left: Detector signal of a nanosecond pulsed laser as a function of time; right: characterization of a grating in Littrow configuration without obscuration from the detector.

Using even shorter light pulses also allows investigating the scattering of entire optical systems and with this a differentiation of scattering contributions from different components in an optical system based on the different path lengths and thus time differences of the scattered light.

### 4.3. Light scattering from optical systems

Characterizing the scattering of assembled optical systems is a valuable step to cross-check the results and assumptions made during ray-tracing simulations. This however increases the complexity of scattering measurements as illustrated in Figure 12 for a grism.

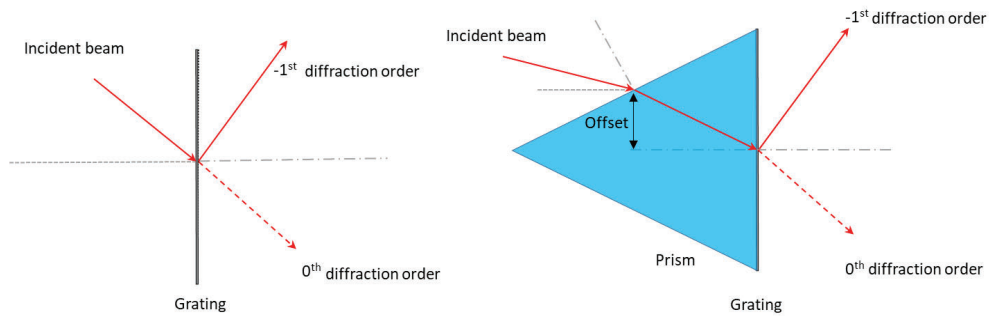


Figure 12: Light scattering measurement of a single optical element (left) and optical system (right).

For the characterization of the grating, the illumination position and coordinate origin for the scattering geometry fall on top of each other. The introduction of the prism however leads to a lateral shift of these two positions, which requires an independent illumination that loosens the usual direct connection between illumination and scattering geometry within a scatterometer as shown in Figure 13.

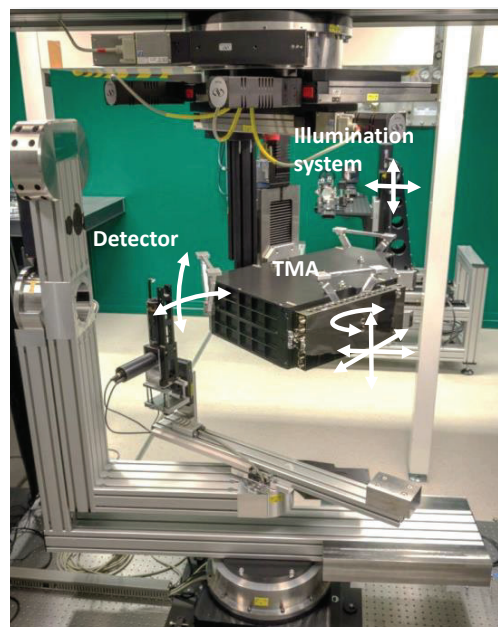


Figure 13: 3D Scatterometer MLS10 with three separate coordinate systems for the illumination, sample (in this case a TMA) and detector.

An application example, where this technique was used is shown in **Fehler! Verweisquelle konnte nicht gefunden werden.**, which shows the scattering of a grating as well as the same grating after it has been bonded to a prism. In both measurement configurations, scattering maps of the grating surface were obtained, by laterally scanning the grating surface at a fixed angle of incidence and scattering. These plots reveal an increase of the scattering distribution, which is natural because of the larger number of interfaces. These maps also reveal some fluctuations over the sample surface, which are hard to simulate in an optical ray-tracer because of the missing input information.

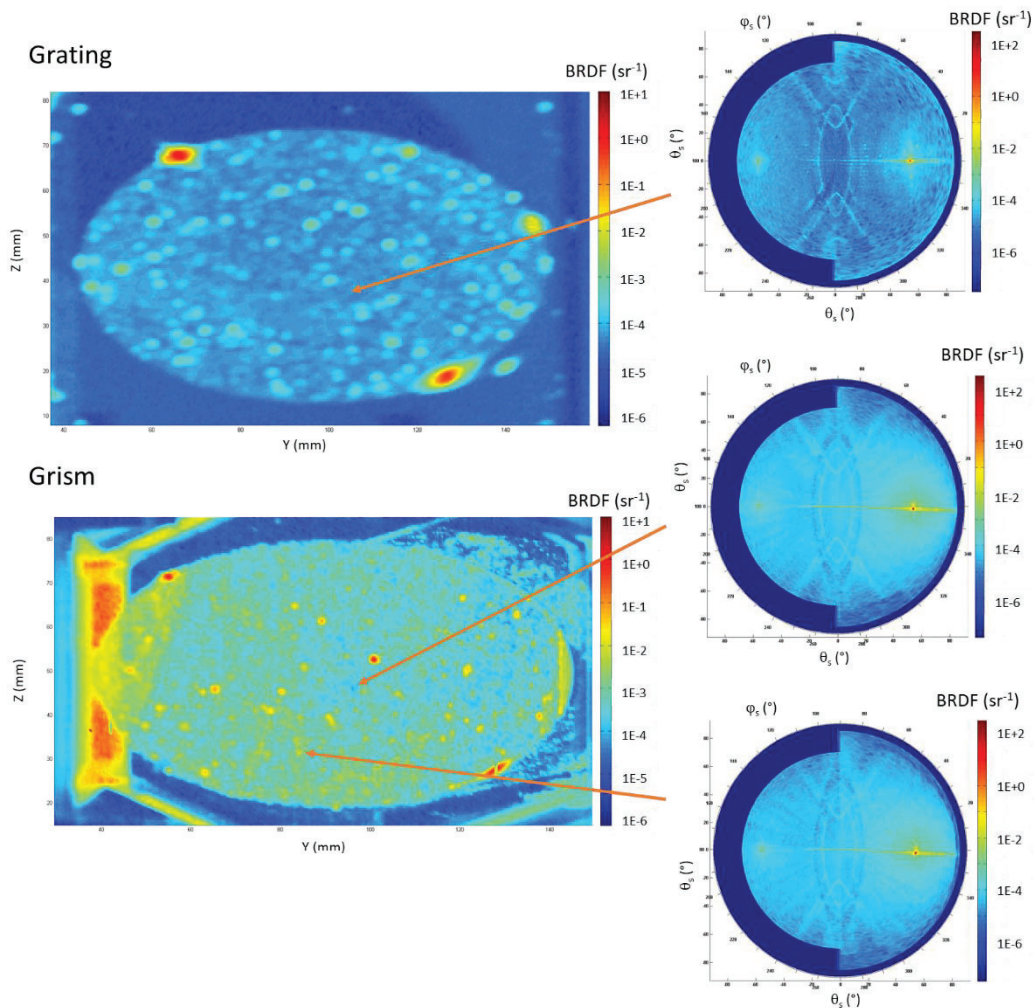


Figure 14: Light scattering mappings of a single grating (top) and grism (bottom) with 3D scattering distribution at different positions on the samples. The use order of the grating is at  $\theta_s = 54^\circ$  and  $\varphi_s = 0^\circ$ .

At different positions, the 3D scattering distribution is recorded as it will later be partly seen by the detector. These plots show very fine details in the scattering distribution. The calculation of the encircled energy around the use order of the grating / grism as shown in Figure 15 can be directly used to determine the unwanted but always present scattering on the detector array, which directly impacts the spectral purity of the later spectrometer.

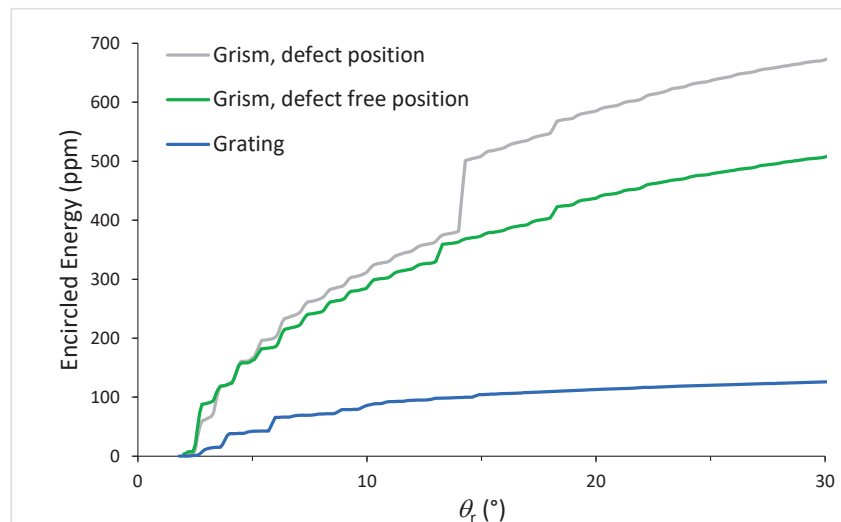


Figure 15: Encircled energy around the use order of the grating for scattering angles  $\theta_r > 2^\circ$ .

## 5. CONCLUSION

Light scattering is caused by even small imperfections and is thus always present but unwanted in optical systems. This high sensitivity however makes light scattering measurements a very powerful characterization tool that helps pushing fabrication limits further and further, which also generates new challenges on scattering metrology such as measurement very close to the specular beam direction, characterization of assembled optical components, measurements under Littrow configuration or in retro-reflex direction. It was shown how aberration-corrected optics can be used to characterize the scattering distribution as close as  $0.05^\circ$  to the specular beam direction even of high-quality optics. It was also demonstrated how time-resolved light scattering measurements enable the characterization of the scattering distribution at angles where it is usually obscured from the detector and how an independent illumination concept of a scatterometer enables the characterization of optical systems consisting of more than one optic.

## ACKNOWLEDGEMENTS

The authors would like to thank the light scattering team at Fraunhofer IOF for the setup and continuous improvement of the measurement equipment and the support during the measurements. Nils Heidler (Fraunhofer IOF) is gratefully acknowledged for providing high-quality samples.

## REFERENCES

- [1] E. L. Church, H. A. Jenkinson, and J. M. Zavada, "Relationship Between Surface Scattering and Microtopographic Features," *Opt. Eng.* 18, 125 (1979).
- [2] J. C. Stover, *Optical Scattering: Measurement and Analysis* (SPIE Press, Bellingham, Wash., USA, 2012), 3rd ed.
- [3] M. Zerrad and M. Lequime, "Instantaneous spatially resolved acquisition of polarimetric and angular scattering properties in optical coatings," *Appl. Opt.* 50, C217-C221 (2011).
- [4] T. A. Germer and C. C. Asmail, "Goniometric optical scatter instrument for out-of-plane ellipsometry measurements", *Rev. Sci. Instrum.* 70, 3688 (1999).
- [5] S. Schröder, T. Herffurth, M. Trost, and A. Duparré, "Angle-resolved scattering and reflectance of extreme-ultraviolet multilayer coatings: measurement and analysis", *Appl. Opt.* 49, 1503-1512 (2010).
- [6] A. von Finck, M. Hauptvogel, and A. Duparré, "Instrument for close-to-process light scatter measurements of thin film coatings and substrates," *Appl. Opt.* 50, C321-C328 (2011).

- [7] S. Schröder, D. Unglaub, M. Trost, X. Cheng, J. Zhang, and A. Duparré, "Spectral angle resolved scattering of thin film coatings," *Appl. Opt.* 53, A35-A41 (2014)
- [8] F.E. Nicodemus, J.C. Richmond, J.J. Hsia, I. W. Ginsberg, and T. Limperis, "Geometrical Considerations and Nomenclature for Reflectance," U. S. Dept. of Commerce, October 1977.
- [9] ISO 19986:2020, Lasers and laser-related equipment — Test method for angle resolved scattering (2020).
- [10] S. Schröder, A. von Finck, and A. Duparré, "Standardization of light scattering measurements," *Adv. Opt. Techn.* 4, 361-375 (2015).
- [11] M. Trost and S. Schröder; "Roughness and Scatter in Optical Coatings" in "Optical Characterization of Thin Solid Films" O. Stenzel and Ohlídal M., eds (Springer Series in Surface Sciences 2018).
- [12] ISO 13696:2002(E), Optics and optical instruments - Test methods for radiation scattered by optical components (2002).
- [13] T. Herffurth, S. Schröder, M. Trost, A. Duparré, and A. Tünnermann "Comprehensive nanostructure and defect analysis using a simple 3D light-scatter sensor," *Appl. Opt.*, Vol. 52, 3279-3287 (2013).
- [14] M. Trost, S. Schröder, T. Feigl, A. Duparré, and A. Tünnermann, "Influence of the substrate finish and thin film roughness on the optical performance of Mo/Si multilayers," *Appl. Opt.* 50, C148-C153 (2011).
- [15] M. Trost, T. Herffurth, S. Schröder, A. Duparré, M. Beier, S. Risse, A. Tünnermann, and N. R. Bowering, "In situ and ex situ characterization of optical surfaces by light scattering techniques," *Opt. Eng.* 53, 092013 (2014).
- [16] A. Duparré and D. Ristau, "Optical interference coatings 2010 measurement problem," *Appl. Opt.* 50, C172–C177 (2011).
- [17] T. Herffurth, M. Trost, M. Beier, R. Steinkopf, N. Heidler, T. Pertermann, and S. Schröder, "Assessing surface imperfections of freeforms using a robotic light scattering sensor," *Opt. Eng.* 58, 092609 (2019).
- [18] J. C. Stover, "Scatterometers," in "Handbook of optics: Devices, Measurements, & Properties," M. Bass, ed. (McGraw-Hill, Inc., New York, N.Y., USA, 1995).